In utero transplantation of adult bone marrow decreases perinatal lethality and rescues the bone phenotype in the knockin murine model for classical, dominant osteogenesis imperfecta

Cristina Panaroni,[1,2] Roberta Gioia,[3] Anna Lupi,[3] Roberta Besio,[3] Steven A. Goldstein,[4] Jaclynn Kreider,[4] Sergey Leikin,[5] Juan Carlos Vera,[5] Edward L. Mertz,[5] Egon Perilli,[6] Fabio Baruffaldi,[6] Isabella Villa,[7] Aurora Farina,[8] Marco Casasco,[8] Giuseppe Cetta,[3] Antonio Rossi,[3] Annalisa Frattini,[1,2] Joan C. Marini,[9] Paolo Vezzoni,[1,2] and Antonella Forlino[3]

[1]ITB-CNR, Milan, Italy; [2]Istituto Clinico Humanitas, Rozzano, Italy; [3]Department of Biochemistry, University of Pavia, Italy; [4]Orthopedic Research Laboratories, University of Michigan, Ann Arbor; [5]Section on Physical Biochemistry, National Institute of Child Health and Human Development (NICHD), National Institutes of Health (NIH), Bethesda, MD; [6]Laboratorio di Tecnologia Medica, Istituti Ortopedici Rizzoli, Bologna, Italy; [7]Bone Metabolic Unit San Raffaele Scientific Institute, Milan, Italy; [8]Department of Experimental Medicine, Section of Histology and Embryology, University of Pavia, Pavia, Italy; and [9]Section on Connective Tissue Disorders, Bone and Extracellular Matrix Branch (BEMB), NICHD, NIH, Bethesda, MD

Autosomal dominant osteogenesis imperfecta (OI) caused by glycine substitutions in type I collagen is a paradigmatic disorder for stem cell therapy. Bone marrow transplantation in OI children has produced a low engraftment rate, but surprisingly encouraging symptomatic improvements. In utero transplantation (IUT) may hold even more promise. However, systematic studies of both methods have so far been limited to a recessive mouse model. In this study, we evaluated intrauterine transplantation of adult bone marrow into heterozygous BrtlIV mice. Brtl is a knockin mouse with a classical glycine substitution in type I collagen [α1(I)-Gly349Cys], dominant trait transmission, and a phenotype resembling moderately severe and lethal OI. Adult bone marrow donor cells from enhanced green fluorescent protein (eGFP) transgenic mice engrafted in hematopoietic and nonhematopoietic tissues differentiated to trabecular and cortical bone cells and synthesized up to 20% of all type I collagen in the host bone. The transplantation eliminated the perinatal lethality of heterozygous BrtlIV mice. At 2 months of age, femora of treated Brtl mice had significant improvement in geometric parameters ($P < .05$) versus untreated Brtl mice, and their mechanical properties attained wild-type values. Our results suggest that the engrafted cells form bone with higher efficiency than the endogenous cells, supporting IUT as a promising approach for the treatment of genetic bone diseases. (Blood. 2009;114:459-468)

Introduction

Osteogenesis imperfecta (OI) has long been considered a paradigmatic disorder for bone marrow or isolated mesenchymal stem cell (MSC) transplantation for skeletal dysplasias.[1] Severe forms of OI are characterized by extreme bone fragility, fractures, skeletal deformities, and short stature; some severe cases are lethal in the perinatal period. The most common molecular defect in OI is a mutation in *COL1A1* or *COL1A2*, encoding the α1(I) and α2(I) chains of type I collagen, respectively.[2,3] Surgical reconstruction, bisphosphonate administration, and physical therapy are interventions often used to treat patients with OI, but these approaches yield limited functional improvements.[4-6] Attempts at gene therapy intervention with antisense oligonucleotides, small interfering RNA (siRNA), ribozymes, or homologous recombination are currently limited to in vitro or ex vivo studies.[7,8] No cure is available.

Importantly, mosaic carriers of OI mutations experience mild to no clinical symptoms, suggesting that even a minor fraction of normal osteoprogenitor cells may have significant clinical benefits.[9] In clinical trials of bone marrow transplantation (BMT) with[10,11] or without[12] isolation of MSCs, Horwitz et al reported just 1% to 2% engraftment in children with OI, but an increase in bone mineral content by DEXA. Subsequently, Le Blanc et al achieved 7% engraftment after in utero transplantation (IUT) of fetal liver donor cells, but any potential phenotypic effects in the patient were masked by bisphosphonate administration.[13] While promising, the results of these human trials are difficult to interpret because of inherent limitations, such as a lack of matched controls and unfeasibility of evaluating engraftment beyond a single biopsy site.

Murine models bypass these limitations, providing not only statistical evaluations of the treatment efficacy, but also better understanding of the engraftment distribution, of the functional status of engrafted cells, and potential side effects. The first BMT for murine OI was performed on a transgenic mouse with a human *COL1A1* minigene and resulted in increased collagen and mineral content in bone.[14] Nyibizi et al reported 0.3% to 28% engraftment in bone after transplantation of newborn *oim* mice with single cells derived from bone marrow osteoprogenitors transduced with a green fluorescent protein (GFP) expressing retrovirus and expanded in culture.[15] Recently, Guillot et al reported approximately 5% engraftment and skeletal improvements after IUT of *oim* mice with fetal MSCs derived from human first trimester blood and transfected with a lentiviral vector expressing enhance GFP (eGFP).[16] Unfortunately, most animal studies were limited to the treatment of *oim* mice with virally transduced cells.[15-17] Viral transduction may alter the differentiation, proliferation, and function of transplanted cells in vivo.[18] In addition, the *oim* mouse itself

Submitted December 20, 2008; accepted April 27, 2009. Prepublished online as *Blood* First Edition paper, May 4, 2009; DOI 10.1182/blood-2008-12-195859.

The online version of this article contains a data supplement.

The publication costs of this article were defrayed in part by page charge payment. Therefore, and solely to indicate this fact, this article is hereby marked "advertisement" in accordance with 18 USC section 1734.

is a model of a rare, recessive form of OI with only one known patient.[19] The results obtained in these studies are difficult to extrapolate and implement into a practical treatment of more common OI forms with dominant transmission.

To develop a more clinically relevant and straightforward model, we performed IUT of heterozygous BrtlIV mice with bone marrow from transgenic mice expressing eGFP. The BrtlIV mouse was developed earlier by a knockin G1546 T transversion in one col1a1 allele, resulting in a Gly349Cys substitution in the α1(I) chain.[20] Substitution of an obligate glycine, found in every third residue of the helical regions of both type I collagen chains, is by far the most common cause of dominant OI.[2,21] The BrtlIV mouse has the typical molecular defect, autosomal dominant transmission, and outcomes resembling human patients.[20]

IUT of adult bone marrow or bone marrow-derived MSCs may be advantageous compared with other stem cell treatments. Fetal stem cells may be tumorigenic,[22-24] and their use may be limited by ethical concerns.[25] Adult bone marrow contains progenitor cells for hematopoietic and mesenchymal lineages;[1,26,27] transplantation of these cells may be particularly beneficial in disorders such as OI, in which only limited lineages need to be replaced or restored.[28] IUT is considered more risky than postnatal BMT, but it may be the only option for preventing early organ failure or fetal mortality, and it may have other advantages.[29] An immunologically immature fetus may accept foreign antigens, thus eliminating the need for conditioning therapy before the transplantation.[30,31] In addition, the small fetal size may obviate the transplantation of large cell numbers and the high proliferative capacity and exponential cellular expansion during fetal development may facilitate the migration of stem cells to different anatomic compartments. All these factors may simplify donor selection and decrease the requirement for human leukocyte antigen (HLA)–matching, as well as allowing smaller graft size.

In the present study, we measured the cell engraftment in various tissues and the mineral content, geometry, and mechanical properties of bones. However, these well-established parameters may not reveal whether the observed effects are actually caused by the engrafted cells rather than the transplantation process itself.[18] To address this question, we went beyond previous approaches and analyzed the proportions of bone matrix synthesized by the host and engrafted cells, as well as the matrix properties near cells of each origin. This study revealed surprising evidence of higher matrix synthesis activity by donor cells, suggesting that even a relatively low engraftment may offer significant therapeutic benefits for OI and potentially for other bone disorders.

Methods

Animals

The mouse model for OI, BrtlIV (129SvJ, C57BL/6, CD1), used for this study was described previously.[20] Cytomegalovirus (CMV)/eGFP CD-1 transgenic mice, in which the eGFP gene is controlled by the CMV promoter/enhancer, were used to obtain donor cells; these mice were a kind gift from Dr Masaru Okabe (Osaka University, Osaka, Japan).[32] The use of mice was approved by the local Pavia City Hall authorities (reference no. 7287/00) and by the Italian Ministry of Health according to Art. 12, D.L. 116/92.

IUT

Fresh bone marrow was obtained from hind limbs of 6- to 8-week-old CMV/eGFP CD-1 transgenic mice as described by Dobson et al.[33] Briefly, femora and tibiae were dissected, cleaned of connective tissue, and placed on ice in phosphate-buffered saline (PBS) solution (1×; Sigma-Aldrich) supplemented with 2% fetal bovine serum (FBS; Euroclone). After clipping off the epiphysis, the bones were centrifuged in specialized tubes for 1 minute at 400*g* to collect the marrow.[34] Each pellet was resuspended in 0.4 mL PBS with 2% FBS using a 23-gauge syringe. The marrow obtained from each animal was pooled in one 15-mL tube and centrifuged at 450*g*. The pellet was resuspended in 1 mL ACK lysing buffer (Sigma-Aldrich) for 5 minutes at room temperature. After additional pelleting, the cells were resuspended in PBS, 2% FBS, passed through a 40-μm nylon mesh filter (Millipore), and counted.

Pregnant wild-type (WT) females crossed with BrtlIV heterozygous males underwent allogenic IUT at embryonic day (E) 13.5 to E14.5. A midline laparotomy was performed on anesthetized females, and the uterine horns were exteriorized. Each fetus was injected intrahepatically with 6 μL suspension containing 5×10^6 cells through a glass capillary.[35] Uterine horns were replaced, and the wound was closed with absorbable synthetic sutures and staples. The animals were genotyped by polymerase chain reaction (PCR) using genomic DNA from tail biopsies.[36]

Tissue examination by fluorescence and confocal microscopy

Spleen, thymus, liver, lung, brain, pancreas, kidney, fat, testis, and calvarial bone from killed mice were examined by DMIL-Leica fluorescence microscope (Leica). Mice containing $eGFP^+$ cells were used for subsequent studies.

For confocal imaging, long bones from 11 WT and 9 Brtl mice were dissected, cleaned of connective tissues, and fixed in 4% paraformaldehyde (PFA; Sigma-Aldrich) in PBS for 24 hours. The bones were then decalcified in 14% ethylenediaminetetraacetic acid (EDTA)/PBS, pH 7.1, for 4 days[37] and incubated in 30% sucrose/PBS for 24 hours. All procedures were performed at 4°C in the dark. Bone samples were embedded in optimal cutting temperature compound (OCT; Tissue-Tek, Sakura Finetek), and 10-μm cryosections were cut onto superfrost Plus Gold Slides (Thermo Fisher Scientific). The nuclei were counterstained by 4′,6-diamidino-2-phenylindole (DAPI; 0.5 μg/mL). The sections were examined by TCS SP2-Leica confocal microscope (Leica).

Fluorescence-activated cell sorting

Suspensions of cells isolated from bone marrow, spleen, and peripheral blood were analyzed by a FACScanto I and II flow cytometers (Becton Dickinson France SAS), using the FACSDiva software supplied by the manufacturer. At least 50 000 events per sample were counted. The cells of donor origin were counted by setting the eGFP fluorescence emission threshold above the endogenous fluorescence level in cells from age-matched untreated mice.

The composition of MSCs and precursor stromal cells in transplanted animals was investigated by 4-color sorting for eGFP, monoclonal phycoerythrin (PE)–conjugated anti-CD117 (eBioscience), monoclonal allophycocyanin (APC)–conjugated anti-Sca1 (eBioscience), and Lineage-negative (Lin^-) cells,[38] using the Lineage Cell Depletion Kit (Miltenyi Biotec) with the Streptavidin-Peridinin Chlorophyll-α Protein (SAv-PerCP; BD Pharmingen, BD Biosciences). At least 70 000 live cells were acquired for each sample. To evaluate the hematopoietic chimerism in the blood, bone marrow, and spleen, the following monoclonal antibodies were used: PE-conjugated anti-Ter119 and anti-CD11b (BD Pharmingen), PE-Cy7–conjugated anti-CD45 (eBioscience), PerCP-conjugated anti-B220, and APC-conjugated anti-CD3 and Ly-G6 (Gr-1; BD Pharmingen) for erythroid and myeloid cells, all hematopoietic cells excluding mature erytrocytes and platelets, B lymphocytes, T lymphocytes, and granulocytes, respectively.

Real-time PCR

Total DNA was extracted from fat, spleen, liver, bone marrow, thymus, skin, lung, muscle, and brain tissue samples, as well as from entire long bones and calvariae, by cellular lysis and isopropanol precipitation.[39] Real-time PCR assays for mouse albumin and eGFP were performed using 25-μL reaction mixtures with 12.5 μL SYBR Green Master mix (Applied Biosystems) and 300 ng DNA template.[15] The eGFP (GenBank accession

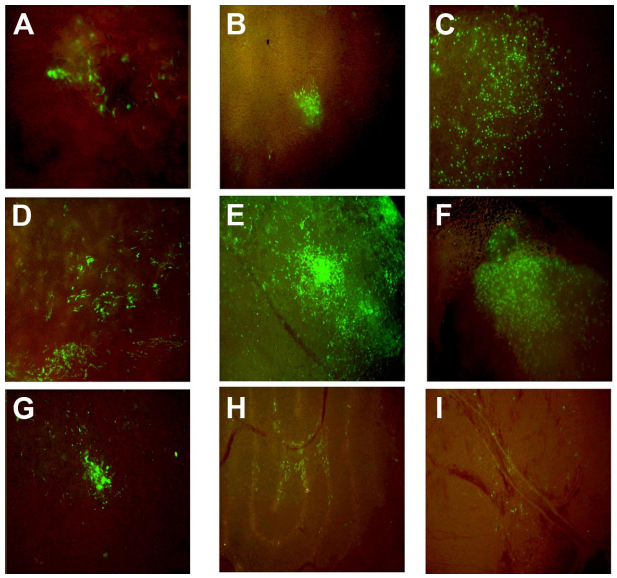

Figure 1. Distribution of eGFP$^+$ cells in hematopoietic and nonhematopoietic tissues in recipient mice at 2 months posttransplantation. (A) Calvarial bone, (B) liver, (C) lung, (D) spleen, (E) pancreas, (F) thymus, (G) fat, (H) testis, and (I) brain are shown. The samples were collected from transplanted animals at sacrifice and imaged in a DMIL-Leica fluorescence microscope with DFC480-Leica camera and 10×/0.22 NA objective.

no. AB205478) forward and reverse primers were 5′-TCCAGGAGCGCACCATCTT-3′ (851-869 bp) and 5′-TGCCGTTCTTCTGCTTGTCG-3′ (1035-1054 bp), correspondingly. The mouse albumin (GenBank accession no. AK050248) forward and reverse primers were 5′-GAAAACCAGGCGACTATCTCCA-3′ (903-924 bp) and 5′-TGCACACTTCCTGGTCCTCA-3′ (1037-1056 bp). The reaction was cycled 40 times for 30 seconds at 94°C, 30 seconds at 60°C, and 30 seconds at 72°C. Standard curves were generated by serial 10-fold dilutions of eGFP (208 bp) and albumin (154 bp) fragments subcloned into TA Cloning vector (Invitrogen). The relative quantitative values of the target eGFP gene were normalized to the endogenous albumin gene. The results were expressed as percent of eGFP$^+$ control for each examined tissue.

Peripheral quantitative computed tomography

Peripheral quantitative computed tomography (pQCT) measurements were performed using a Stratec Research SA$^+$ pQCT scanner (Stratec Medizintechnik GmbH) with 70 μm voxel size and 3 mm/second scan speed. To orient the long axes of the bones parallel to the image planes, the excised bone specimens were fixed with manufacturer-made plastic holders. The correct longitudinal positioning was determined from an initial "scout scan." The scans were performed at the distal metaphysis of tibiae, proximal metaphysis of femora, and diaphysis of both bones. The scans were analyzed with pQCT software 6.00B using contour mode 2 and peel mode 2 with a threshold of 350 mg/cm^3 for trabecular and total bone and with a threshold of 600 mg/cm^3 for cortical bone.

Microcomputed tomography

Left femora from male BrtlIV mice and their WT littermates, with or without IUT, were scanned on a cone beam micro-computed tomography (microCT) system (eXplore Locus SP; GE Healthcare BioSciences). The images were calibrated and reconstructed at 10 μm voxel size. Standardized femoral mid-diaphyseal cortical regions of interest were isolated, thresholded, and assessed structurally and densitometrically (Microview ABA; GE Healthcare BioSciences). Trabecular compartments within the distal metaphysis of the femur were also isolated, thresholded, and evaluated for morphologic and densitometric measures (Microview ABA).

Mechanical testing

Whole-bone mechanical properties were determined by loading the left femora to failure in 4-point bending using a servohydraulic testing machine (858 Mini Bionix II; MTS Systems) at a constant displacement rate of 0.5 mm/s. Femora were loaded in the anterior-posterior direction with the posterior side in tension and the anterior side in compression. Load-displacement curves were analyzed with MATLAB 7.1 software (Mathworks). Bone tissue material properties were predicted using standard mechanics of material equations, assuming a bending mode of failure. Data for each microCT outcome measure were assessed with independent sample *t* test using SPSS version 16.1 (SPSS). Separate models were used for different genotypes.

Colony-forming units fibroblasts (CFU-F)

Bone marrow cells were isolated from hind limbs of transplanted 2-month-old mice as described above, and 10^7 cells were plated in a 6-well plate (Costar, Corning) in Mesencult medium with supplement (Biocompare). The medium was replaced after 24 hours. Plastic adherent stromal cells from Brtl and WT treated mice were grown for 1 week, changing the medium twice. CFU-F colonies were stained by Giemsa (Sigma-Aldrich)

Table 1. FACS analysis of Lin$^-$/Sca1$^+$/CD117$^-$ cells from 2-month-old treated and untreated mice

Mouse-sex	Genotype	% eGFP$^+$ in bone marrow	%Lin$^-$/Sca1$^+$/CD117$^-$ in bone marrow*	% eGFP$^+$ within Lin$^-$/Sca1$^+$/CD117$^-$ population†
604-F	WT	3.2	0.24	10.4
606-M	BrtlIV	0.91	0.1	3.0
615-F	BrtlIV	0.68	0.31	0.9
1178-F	BrtlIV	0.19	0.3	0.6
1180-M	WT	0.19	0.19	0.3
1181-M	WT	0.38	0.12	0.3
1182-F	WT	0.57	0.12	0.9
1184-F	WT	0.95	0.11	0.4
1187-M	BrtlIV	0.57	0.12	0.9
1188-M	WT	0.57	0.13	0.3
1189-M	BrtlIV	0.57	0.12	0.7
616-M‡	BrtlIV	n.d.	0.35	n.d.
617-M‡	WT	n.d.	0.22	n.d.
623-F‡	BrtlIV	n.d.	0.31	n.d.
1195-F‡	WT	n.d.	0.12	n.d.
1197-F‡	BrtlIV	n.d.	0.17	n.d.

F indicates female; and M, male.
*The percentage refers to the total cell population.
†The percentage refers to the Lin$^-$/Sca1$^+$/CD117$^-$ compartment.
‡Untreated mice.

Table 2. FACS analysis of peripheral blood, spleen, and bone marrow cells from 2-month-old recipient mice (IUT, n = 9) and untreated animals (No IUT, n = 4)

	Peripheral blood		Spleen		Bone marrow	
	IUT	No IUT	IUT	No IUT	IUT	No IUT
% $CD45^+$	97.7 ± 3.3	91.6 ± 4.5	79.0 ± 6.9	85.6 ± 5.9	69.6 ± 6.1	74.3 ± 1.3
% $eGFP^+$ in the lineage	1.35 ± 0.77	n.d.	0.6 ± 0.26	n.d.	0.38 ± 0.19	n.d.
% $CD3^+$	33.7 ± 5.2	28.1 ± 2.6	23.2 ± 3.1	21.3 ± 2.2	1.21 ± 0.22	0.85 ± 0.35
% $eGFP^+$ in the lineage	1.08 ± 0.74	n.d.	0.77 ± 0.44	n.d.	0.98 ± 0.60	n.d.
% $B220^+$	36.7 ± 8.3	47.6 ± 4.9	69.9 ± 7.6	82.0 ± 6.6	26.1 ± 5.6	36.9 ± 5.9
% $eGFP^+$ in the lineage	0.32 ± 0.22	n.d.	0.51 ± 0.22	n.d.	0.35 ± 0.12	n.d.
% $CD11b^+$	20.2 ± 5.9	14.1 ± 2.83	7.6 ± 2.2	5.9 ± 0.78	37.5 ± 7.0	32.7 ± 9.8
% $eGFP^+$ in the lineage	4.2 ± 3.1	n.d.	0.6 ± 0.85	n.d.	0.79 ± 0.52	n.d.
% Ly-6G(Gr-1)$^+$	15.4 ± 5.7	9.7 ± 2.6	3.0 ± 1.4	1.8 ± 1.1	27.5 ± 6.0	24.1 ± 8.4
% $eGFP^+$ in the lineage	5.2 ± 4.2	n.d.	1.3 ± 0.49	n.d.	0.58 ± 0.43	n.d.
% $Ter119^+$	37.3 ± 3.2	43.1 ± 3.6	20.6 ± 6.6	14.3 ± 6.5	29.5 ± 6.5	21.2 ± 5.7
% $eGFP^+$ in the lineage	1.71 ± 0.81	n.d.	1.77 ± 0.87	n.d.	4.0 ± 4.2	n.d.

The antigens used to identified the lineages were CD45 for hematopoietic cells, CD3 for T lymphocytes, B220 for B lymphocytes, CD11b for myeloid cells, Ly-G6 (Gr-1) for granulocytes, and Ter119 for erythroid cells. For each lineage marker, the first line shows the mean fraction of positive cells (percentage) ± SD. The second line shows the engraftment of $eGFP^+$ cells within the lineage. n.d. indicates not determined.

and analyzed with fluorescence and light microscopy. Only colonies containing more than 50 cells (all $eGFP^+$) were considered positive.

Osteoblast primary cultures

Femora of transplanted mice were cleaned of soft tissue, the metaphyses were removed, and the marrow flushed out with cold PBS. Osteoblasts were established according to the Robey and Termine method.[40] Briefly, osteoblasts were released by digesting bone chips for 2 hours at 37°C with 0.3 U/mL collagenase P in serum-free medium, then grown in α-minimum essential medium (MEM) containing 25 μg/mL ascorbate, 2 mM glutamine, and 10% FBS in presence of 5% CO_2. Osteoblast cultures were analyzed by fluorescence and light microscopy.

Collagen analysis

Trabecular and cortical bone from the interface between the diaphysis and metaphysis were dissected from the distal end of the femur. The residual soft tissue was removed after loosening by partial digestion with 1 mg/mL trypsin (Sigma-Aldrich) in Dulbecco PBS (DPBS) with calcium and magnesium at 4°C for several days. Cleaned trabeculae and cortical pieces were separated, demineralized in 0.5 M EDTA for 1 week at 4°C, and washed with water. The demineralized matrix was rendered soluble with 2 doses of 0.5 mg/mL pronase (Calbiochem, EMD Chemicals) in 0.5 M NaCl, 25 mM Tris, 0.05% Brij35 at 4°C. The second dose was added after 3 to 4 days. After 1 week, the reaction was stopped with acetic acid (0.5 M final concentration), and collagen was precipitated by raising the NaCl concentration to approximately 1 M. The precipitated collagen was washed with 70% ethanol, resolubilized in 0.1 M Na-carbonate, 0.5 M NaCl, pH 9.3, fluorescently labeled with Cy5 (Crt Healthcare),[41] and separated on precast, gradient, Tris-acetate minigels (3%-8%; Invitrogen). The gels were scanned on an FLA5000 fluorescence scanner (Fuji Medical Systems) and analyzed with the ScienceLab software supplied by the manufacturer (Fuji Medical Systems).

Raman microspectroscopy

Bone pieces from femoral diaphyses were fixed in 1% formaldehyde/DPBS for 2 hours at 20°C and cryosectioned at 4 or 15 μm on a Vibratome 5000 Deluxe (Vibratome). The sections were washed with DPBS, optically clarified with saturated CsCl solution, 10 mM 4-(2-hydroxyethyl)-1-piperazine-ethanesulfonic acid (HEPES), pH 7.4, mounted between an A1 fused quartz slide and a coverslip (ESCO Products), and 10 to 15 cm^{-1} resolution Raman spectra were recorded in a Senterra confocal Raman microscope (Bruker Optics) using a 40×/0.95 objective and 50-μm pinhole. Spectral peaks were analyzed after subtracting straight baselines from solution-corrected spectra.

Results

IUT of total bone marrow cells into Brtl and WT embryos

Whole bone marrow cells from long bones of adult CMV/eGFP CD-1 transgenic mice, depleted of red blood cells, were transplanted into livers of E13.5-14.5 embryos from WT females crossed with Brtl males. Although no difference in litter size or in the ability of females to successfully raise pups has been reported for BrtlIV mice, WT dams were chosen to avoid potential delays in recovery from surgery and delivery. The ability of the harvested bone marrow cells to differentiate into osteoblasts and adipocytes was confirmed in vitro by Von Kossa and Oil Red O staining, respectively (supplemental Figure 1, available on the *Blood* website; see the Supplemental Materials link at the top of the online article).

A total of 464 fetuses in 56 WT females were transplanted, 36.4% of which (n = 169) reached the weaning age (3 weeks). Among the latter 51.4% (n = 87) were WT and 48.5% (n = 82) were heterozygous BrtlIV, suggesting nearly equal survival of WT and mutant animals (1:1). In untreated animals from our colony, BrtlIV pups had a survival rate 2 times lower compared with WT and, at the same age of 2 months, 65.5% were WT and 34.5% were heterozygous BrtlIV, consistent with previous reports.[20,41] The significantly higher ($P = .04$) proportion of surviving BrtlIV animals in transplanted mice indicated that the treatment rescued the genotype-related lethality in our murine model.

The genotype-independent lethality of transplanted mice could be caused by accidental tissue damage during the transplantation (due to the small animal size) or inadequate fostering of the litters that had been neglected by the mothers.

Donor cell engraftment in hematopoietic and nonhematopoietic tissues

The transplanted mice were killed at age 2 months, the age at which the Brtl phenotype is most severe compared with WT littermates.[42] Of 135 mice examined, 87 (64.4%) had detectable donor green cells in spleen, thymus, calvarial bone, fat, liver, lung, pancreas, and testis (Figure 1). The percentage of male mice with detectable $eGFP^+$ cells (70.5%, n = 48/68) appeared to be higher than females (58.2%, n = 39/67), but the difference was not statistically

significant ($P = .332$). Similar fractions of mutant and WT mice had eGFP$^+$ cells in their tissues: 64.6% Brtl (n = 21/32) versus 77.7% WT (n = 28/36) males and 58.8% Brtl (n = 20/34) versus 57.5% WT (n = 19/33) females. As previously reported by Dominici et al, the cells were organized in patches, suggesting their clonal origin (Figure 1).[43]

CFU-F colonies positive for Giemsa (46 ± 18) and for Giemsa and eGFP (3 ± 1) were found in bone marrow stromal cell cultures from 2-month-old treated mice, suggesting that transplanted cells remained viable up to 2 months after transplantation and explaining the persistence of eGFPs cells in various organs (supplemental Figure 2). From quantitative analysis by FACS, we found that 0.1% to 10.4% of Lin$^-$/Sca1$^+$/CD117$^-$ (a subset of early progenitor cells[44]) were eGFP$^+$ (Table 1 and see supplemental Figure 3). Hematopoietic chimerism was detected in blood, spleen, and bone marrow as well (Table 2 and supplemental Figure 4).

Further FACS analysis on single-cell suspensions (Figure 2A) revealed eGFP$^+$ cell engraftment from 0.14% to 6.93% (1.52% ± 1.42%, n = 41) in spleen and from 0.21% to 11.56% (1.31% ± 2.29%, n = 30) in bone marrow (Table 3). Lower engraftment was detected in mutant mice (spleen, 1.28% ± 1.19%; bone marrow, 0.75% ± 0.56%) compared with WT (spleen, 1.78% ± 1.62%; bone marrow, 1.95% ± 3.21%), but this trend was not statistically significant due to high engraftment variability.

Quantitation of eGFP genomic DNA by real-time PCR also revealed high engraftment variability among different animals (Figure 3). The highest engraftment was detected in fat and spleen. The engraftment in brain and muscle was below 0.1% in all samples. The engraftment in the full diaphyseal cortical bone was close to that of the bone marrow and consistent with engraftment evaluated in the same animals by FACS (Figure 3 and supplemental Table 1). Thus, the selection of the transplanted mice for further analysis was based on bone marrow FACS measurements.

Engraftment in cortical and trabecular bone

Clusters of eGFP$^+$ cells were detected by confocal microscopy in areas of active bone formation and remodelling in trabeculae and cortical endosteum and periosteum (Figure 2B). Standard osteoblasts cultures from cortical chips of treated mice (Figure 2C) revealed eGFP$^+$ cells with typical osteoblast morphology, coexisting with endogenous eGFP$^-$ cells.

High magnification images of tibial and humeral sections containing eGFP$^+$ cell patches were evaluated from 20 mice. The fraction of donor cells in these sections ranged from 1.18% to 14.59% (6.61% ± 4.19%). No significant difference in the fraction of donor cells was detected between male (7.475% ± 4.911%, n = 12) and female (5.31% ± 2.54%, n = 8) mice ($P > .05$) or between WT (5.05% ± 3.47%, n = 11) and Brtl (8.51% ± 4.61%, n = 9) animals ($P > .05$). Note, however, that this fraction was considerably higher than the overall donor cell engraftment in cortical bone, since many bone sections did not contain eGFP$^+$ cell patches.

Collagen composition in treated and untreated bones from BrtlIV animals

Gel electrophoresis of collagen extracted from trabecular and cortical bones revealed α1(I)-S-S-α1(I) dimers, in addition to α1(I) and α2(I) monomers (Figure 4A). These dimers are formed with more than 95% efficiency in molecules containing 2 mutant α1(I) Gly349Cys chains.[45,46] From the intensities of the α1(I)-S-S-α1(I) and α1(I) bands, we estimated the fraction of collagen molecules

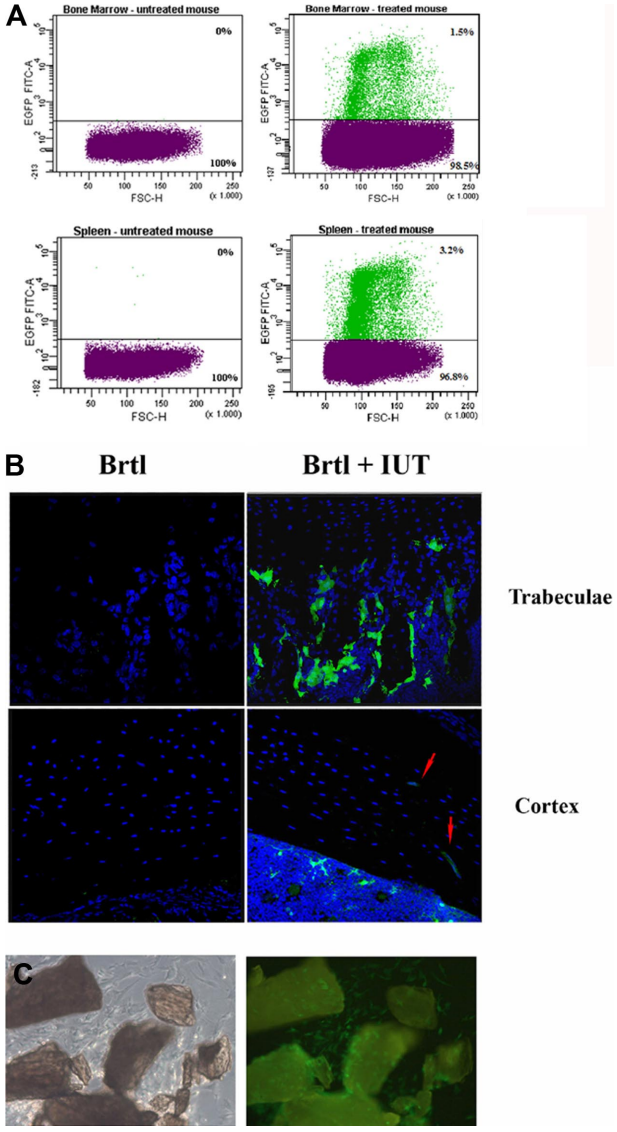

Figure 2. Engraftment analysis by direct cell counting. (A) Example of FACS separation and counting of eGFP$^+$ and eGFP$^-$ cells extracted from bone marrow and spleen of untreated controls (left) and treated mice (right). The sorting gates were set to preferentially select mononuclear cells. The percentage of donor cells was calculated selecting the fluorescent population based on the fluorescence intensity (FL1-H) versus forward scatter (FSC-H). (B) Confocal microscopic images of 10-μm bone sections from untreated (Brtl) and treated (Brtl + IUT) mice. Blue DAPI counterstaining reveals nuclei of all donor and host cells. Green eGFP$^+$ donor cells are visible in the treated sample in the region surrounding the trabeculae at expected locations of osteoblasts and in the cortical region occupied by osteocytes (eGFP$^+$ osteocytes are indicated by red arrows). The imaging was performed in a TCS SP2-Leica confocal microscope with 40×/1.25 NA oil objective; 488 nm excitation and a 500-540 nm emission filter were used for eGFP, and 364 nm excitation and 400-480 nm filter were used for DAPI. (C) Phase contrast (left) and GFP fluorescence (right) images of primary osteoblasts growing from minced femur and tibia chips, obtained with the DMIL-Leica microscope (10×/0.22NA objective).

with 2 mutant chains as 26.7% plus or minus 4.3% in trabecular and 25.7% plus or minus 2.5% in cortical bone from untreated animals, consistent with previous reports.[41,46] In treated animals, this fraction decreased with increasing bone marrow engraftment of donor cells (Figure 4B). In animals with the highest engraftment (1.9% ± 0.1%), this fraction was 20.4% plus or minus 2.9% in trabecular and 20.9% plus or minus 2.6% in cortical bone ($P < .05$; Figure 4 and supplemental Table 2). Assuming a random assortment of collagen chains produced by the host cells, this reduction resulted from normal collagen synthesis by the engrafted cells. The

Table 3. FACS analysis of overall eGFP$^+$ cell engraftment in spleen and bone marrow from 2-month-old BrtlIV and WT recipient mice

	BrtlIV			WT	
Mouse-sex	Spleen % eGFP$^+$	Bone marrow % eGFP$^+$	Mouse-sex	Spleen % eGFP$^+$	Bone marrow % eGFP$^+$
498-F	3.45	1.52	348-F	4.23	11.56
537-F	0.31		353-F	3.21	6.04
543-F	0.16		490-F	1.38	0.89
573-F	0.86	0.21	538-F	0.47	
614-F	0.87	0.68	579-F	0.43	0.21
615-F	0.43	0.68	580-F	0.14	0.21
634-F	0.48	0.24	604-F	6.93	3.2
692-F	1.69	1.86	635-F	0.32	0.24
693-F	1.52	0.93	495-M	1.89	1.01
696-F	3.9	1.86	496-M	2.83	0.83
697-F	0.17	0.23	539-M	0.62	
698-F	2.54	0.93	540-M	1.25	0.34
735-F	0.32	0.69	544-M	0.93	
508-M	1.19	0.32	546-M	0.62	
606-M	3.68	0.91	610-M	0.87	0.23
612-M	0.87	0.46	613-M	2.38	0.46
618-M	0.22	0.23	691-M	2.71	1.86
641-M	0.47	0.24	694-M	1.36	0.23
341-M	2.12		344-M	1.59	
347-M	1.06		352-M	1.41	
545-M	0.62				
Mean ± SD	1.28 ± 1.19	0.75 ± 0.56	Mean ± SD	1.78 ± 1.62	1.95 ± 3.21

F indicates female; and M, male.

corresponding recalculation showed that 1.9% engrafted cells produced 21% plus or minus 6% of all bone collagen (Figure 4C).

Bone analysis by pQCT, microCT, and mechanical testing

pQCT analysis of metaphyseal regions showed that the total long bone mineral density was significantly higher in transplanted mice ($P = .03$). Specifically, the trabecular mineral density in the distal femur increased in 2-month-old mutant transplanted males compared with untreated animals (118.41 ± 18.71 mg/cm^3 vs 97.07 ± 10.98 mg/cm^3, $P = .01$). Similarly, the cortical mineral density in the proximal tibia was higher in treated versus untreated Brtl mice (867.50 ± 54.95 mg/cm^3 vs 790.30 ± 45.72 mg/cm^3, $P < .01$; Figure 5 and Table 4). No statistically significant differences were found in other tested parameters (not shown).

MicroCT revealed an increase in the cortical thickness, area, and mineral content in IUT-treated Brtl and in the cortical thickness and mineral content in IUT-treated WT mice (Figure 6A). The mineral density was improved in Brtl-treated versus untreated femora (997.63 ± 19.36 mg/mL vs 987.84 ± 29.85 mg/mL) without reaching statistical significance, as was the femur length (14.59 ± 0.47 mm vs 14.43 ± 0.54 mm). Importantly, only the Brtl IUT group showed an increase in the yield load (20.5 ± 4.33 N vs 15.57 ± 3.19 N, $P < .05$), ultimate load (28.56 ± 4.97 N vs 20.41 ± 3.68 N, $P < .05$), and stiffness (197.80 ± 52.54 N/mm vs 141.22 ± 30.26 N/mm, $P < .05$) compared with untreated controls. In these animals, the treatment restored the bone mechanics to almost normal compared with WT (Figure 6B). No difference in the bone mechanics was noted between the treated and untreated WT groups (Figure 6B). Interestingly, the predicted strength (109.69 ± 23.97 MPa vs 78.58 ± 18.26 MPa, $P < .05$) was higher in the treated Brtl than in treated or untreated WT mice (Figure 6C).

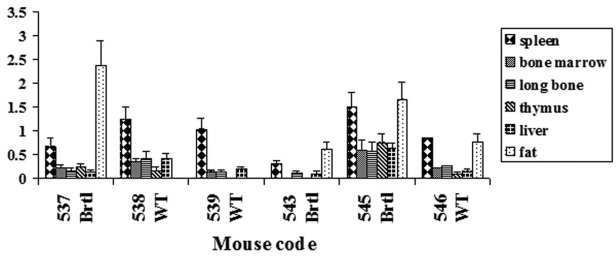

Figure 3. Real-time PCR evaluation of engraftment in different tissues of recipient mice. The amount of eGFP genomic DNA was normalized to albumin genomic DNA. The value of this ratio in eGFP transgenic donor mice was used as a 100% standard. The error bars indicate standard deviation (SD) for each PCR measurement repeated in triplicate.

Microspectroscopic Raman analysis of extracellular matrix mineralization

Samples with eGFP$^+$ osteocytes were selected from approximately 200 longitudinal, radial femur diaphyseal sections from animals with high bone marrow engraftment. Raman spectra were collected from approximately 2-μm spots selected at least 3 μm away from osteocyte lacunae in primary lamellar and primary "fine-fibered"[47] bone. The bone types were classified based on dark-field polarized images of each section, as illustrated in supplemental Figure 5.

We used the integral intensity of $\nu_1PO_4^{3-}$ vibration (924-985 cm^{-1}) as a measure of apatite mineral and the integral intensity of CH stretching (1595-1720 cm^{-1}) or amide I (2842-3030 cm^{-1}) vibrations as independent measures of organic material in the extracellular matrix. The difference in the mineral/matrix ratio near 30 eGFP$^+$ and 66 eGFP$^-$ osteocytes was statistically insignificant ($P = .2$) both within the lamellar and fine-fibered bone, indicating similar average matrix mineralization near host and transplanted cells (Figure 7A). However, the mineral density was significantly less heterogeneous around eGFP$^+$ osteocytes (5.9% ± 1.8% in lamellar and 5.2% ± 0.7% in fine-fibered bone) than around eGFP$^-$ osteocytes (10.0% ± 0.8% and 11.9% ± 1.4%, $P = .016$ and $P = .006$, respectively), as illustrated in Figure 7B.

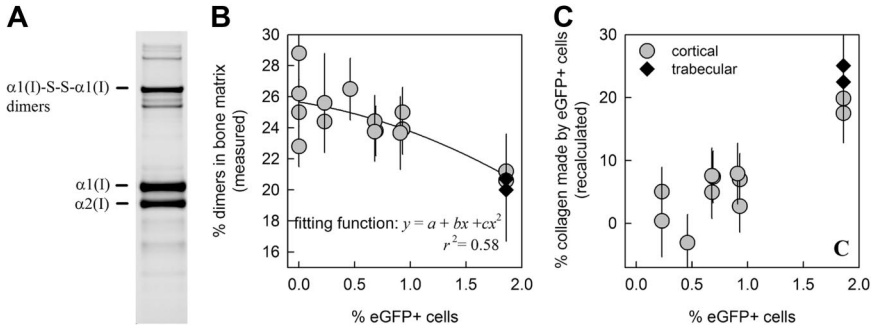

Figure 4. Collagen composition of extracellular matrix in bones from untreated and treated mutant mice. Type I collagen was extracted from trabecular and cortical bone samples and analyzed by quantitative sodium dodecyl sulfate polyacrylamide gel electrophoresis (SDS-PAGE) with fluorescent labeling (A). The fraction of α1(I) chains forming α1(I)-S-S-α1(I) dimers represents the fraction of collagen molecules with 2 mutant chains. This fraction decreased with increasing engraftment of donor (eGFP$^+$) cells ($r^2 = 0.58$) because they produced only collagen without mutant chains (B). Because host cells are expected to synthesize the same fraction of the dimers in treated and untreated animals, the fraction of collagen made by the donor cells (c_d) can be evaluated as $c_d = 1 - d/d_0$, where d and d_0 are the fractions of dimers measured in treated and untreated animals, respectively. This fraction increased with the donor cell engraftment (C, $r^2 = 0.78$). The engraftment was measured for each animal by FACS in bone marrow (Table 3). The same engraftment in the cortical bone is expected from real-time PCR data (Figure 3 and supplemental Table 1).

Discussion

The BrtlIV model of classical, dominant negative OI offers significant advantages for investigating stem cell transplantation compared with the transgenic and recessive *oim* mice previously utilized.[14-17] The primary goal of this work was to define the approach, develop the means, and set the stage for future studies of different treatment aspects. Our observations of (1) a major fraction of bone matrix synthesized by a minor fraction of engrafted osteoblasts, (2) recovery of bone quality in treated mice, and (3) rescue of the lethal phenotype address some existing puzzles and offer insights for future studies.

Engrafted donor cells exhibit more efficient matrix synthesis

The allogenic, intrahepatic transplantation of bone marrow from 1- to 2-month-old transgenic eGFP mice into nonablated E13.5 to E14.5 embryos resulted in 1.35% plus or minus 0.77%, 0.6% plus or minus 0.26%, and 0.38% plus or minus 0.19% engraftment of CD45$^+$ cells in peripheral blood, spleen, and bone marrow, respectively; engraftment was observed in all major hematopoietic lineages (Table 2). Among 0.17% plus or minus 0.08% progenitors (Lin$^-$Sca$^+$CD117$^-$) in the recipient bone marrow, we detected up to 10.4% eGFP$^+$ cells (Table 1). Thus, the transplanted cells maintained their progenitor potential at least through the prepubertal development of host animals, which is the crucial time frame for attainment of peak bone mass. Furthermore, some of these transplanted cells differentiated into mature osteoblasts, which synthesized bone matrix with much higher efficiency than endogenous BrtlIV osteoblasts. Biochemical analysis of femur matrix revealed that 1.9% plus or minus 0.1% of donor osteoblasts produced 21% plus or minus 6% of all bone collagen (Figure 4 and supplemental Table 2). Our interpretation is that donor osteoblasts have normal rather than elevated matrix synthesis efficiency, while the cells of the BrtlIV host have strongly reduced efficiency because of endoplasmic reticulum (ER) stress. Our previous studies of BrtlIV animals have suggested that ER stress and cellular malfunction, associated with accumulation and intracellular degradation of mutant collagen molecules, may be a major factor contributing to the animal phenotype.[41,48]

Low bone engraftment despite noticeable phenotype improvement was observed previously after IUT of human fetal blood MSCs to *oim* mice,[16] after allogenic bone marrow or MSCs transplantation to ablated OI children,[10-12] and after IUT on a 32-week-old human fetus.[13] The dramatically higher matrix synthesis efficiency by engrafted normal cells offers a clue for the understanding these otherwise puzzling observations.

IUT improves bone geometry and mechanical properties

The high matrix synthesis efficiency may explain how 1% to 2% engraftment of donor cells can restore the mechanical properties of bone in BrtlIV animals to nearly normal (Figure 6). We evaluated the changes in bone geometry and mechanics in 2-month-old mice, the age at which the skeletal phenotype of BrtlIV mice is most severe.[42] Similar increases in cortical thickness and area in IUT-treated BrtlIV and WT animals suggested that bone geometry was affected by donor humoral factors or transplantation per se as previously speculated by others.[49]

At the same time, the stiffness, ultimate load, and yield load improved significantly only in BrtlIV animals and not in their WT littermates. More pronounced mechanical benefits of transplantation in BrtlIV animals may result from better matrix quality produced by normal versus BrtlIV cells. Indeed, normal donor cells may be expected to increase matrix quality in BrtlIV animals, but not in their WT littermates, since WT host cells already produce normal matrix. Thus, we investigated local matrix mineralization in

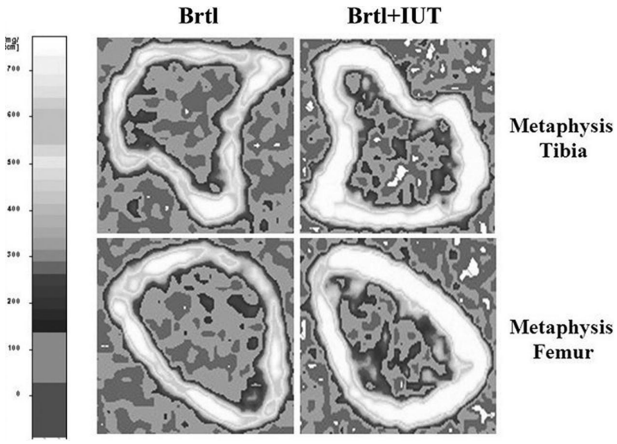

Figure 5. Representative pQCT scans in BrtlIV mice. Shown are scans at the tibial (above) and femoral (below) metaphysis in untreated (left) and treated (right) BrtlIV mice. The treatment induces an increase of bone density at both skeletal sites. The left panel shows the scale of volumetric mineral density.

Table 4. pQCT measurements of the methaphyseal region of distal femur and proximal tibia of untreated (BrtlIV) and treated (BrtlIV plus IUT) mice

	Total density, mg/cm^3	Trabecular density, mg/cm^3	Cortical density, mg/cm^3	Total area, mm^2
Tibia				
BrtlIV	384.94 ± 46.52	116.26 ± 26.67	790.30 ± 45.72	2.68 ± 0.39
BrtlIV plus IUT	444.79 ± 53.80	101.48 ± 18.40	867.50 ± 54.95	2.55 ± 0.38
P	.03	.21	< .01	.54
Femur				
BrtlIV	374.84 ± 56.66	97.07 ± 10.98	851.55 ± 54.08	2.73 ± 0.29
BrtlIV plus IUT	436.61 ± 51.60	118.41 ± 18.71	898.90 ± 57.84	2.83 ± 0.51
P	.03	.01	.10	.63

Values are expressed as mean ± SD.

the vicinity of each cell type by Raman microspectroscopy (Figure S5). The average mineral density was similar, but matrix near the donor cells had a more homogeneous mineral distribution, suggesting that it was also better organized than the matrix produced by the host BrtlIV cells (Figure 7).

IUT rescues the lethal phenotype

Probably the most surprising finding was that the treatment completely prevented the characteristic perinatal lethality of Brtl mice. Treated mice had a Mendelian 1:1 ratio of BrtlIV and WT littermates at 2 months of age, in comparison to the 1:2 genotype ratio in our untreated animals. We hypothesize that donor cells may rescue lethal animals not only by producing better matrix, but also by secreting crucial humoral factors and relieving the ER stress and reducing apoptosis of host cells, due to increased synthesis of normal collagen. The lethal phenotype rescue presents an appealing argument in favor of further development of IUT as a potentially important clinical approach.

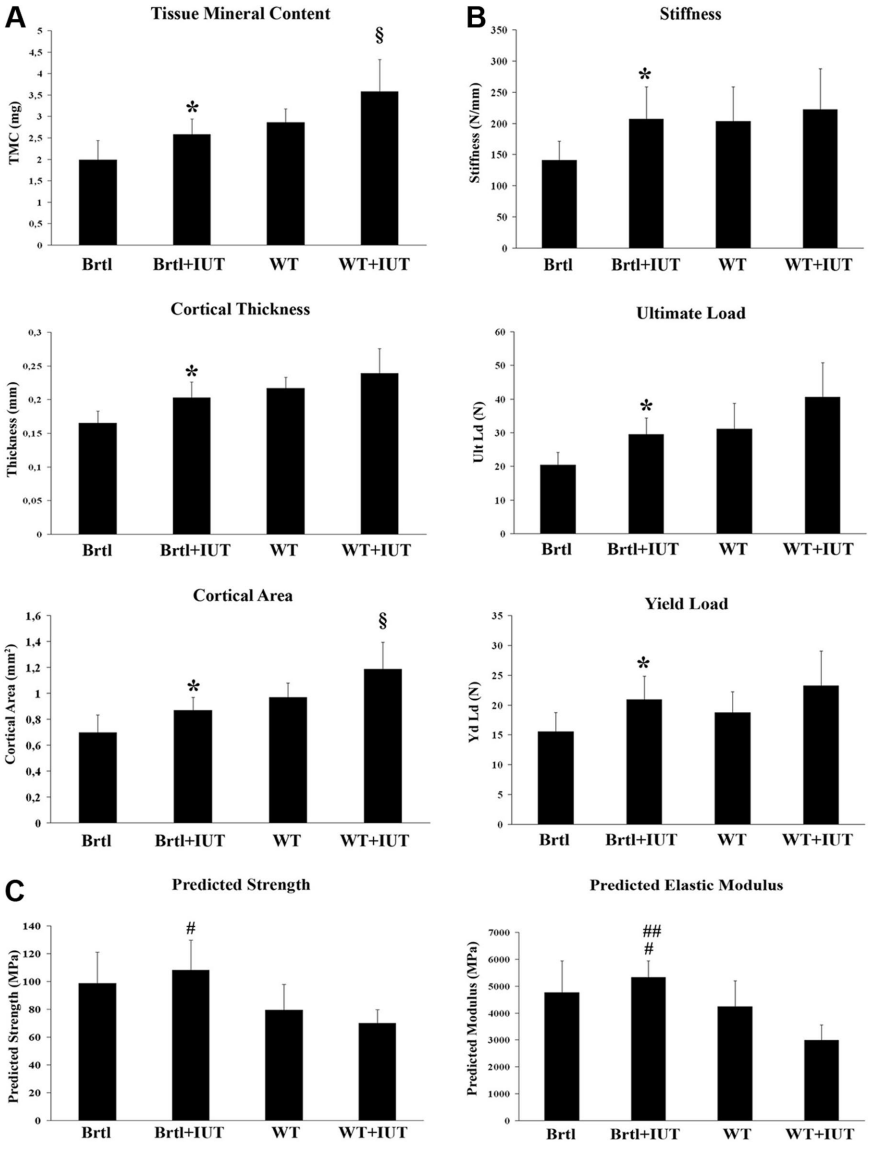

Figure 6. Effect of IUT on geometry and mechanical properties of femurs. (A) Geometric parameters (microCT) of femur in 2-month-old mutant untreated (Brtl, n = 8), mutant treated (Brtl + IUT, n = 12), WT untreated (n = 11), and WT treated (n = 5) mice. (B) Mechanical properties (4-points bending test) of femur in 2-month-old mutant untreated (Brtl, n = 8), mutant treated (Brtl + IUT, n = 5), WT untreated (n = 11), and WT treated (n = 5) mice. (C) Predicted Ultimate Strength and Predicted Elastic Modulus. Bars on graphs are mean ± SD. *$P < .05$ for Brtl + IUT vs Brtl; §$P < .05$ for WT + IUT vs WT, Brtl + IUT; #$P < .05$ for Brtl + IUT vs WT and WT + IUT; and ##$P < .05$ for Brtl + IUT vs WT + IUT.

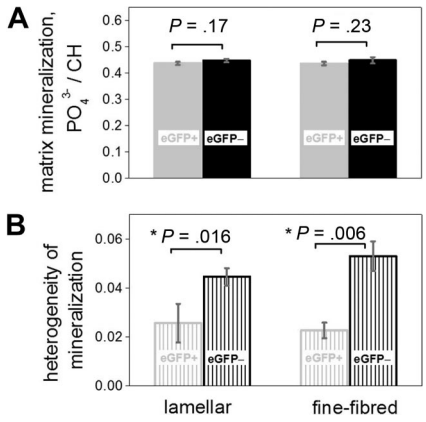

Figure 7. Extracellular matrix mineralization and its heterogeneity near donor eGFP$^+$ and host eGFP$^-$ osteocytes measured by confocal Raman microspectroscopy. The measurements of extracellular matrix mineralization (A) and its heterogeneity (B) were performed near 96 cells in 20 different sections of femur cortical bone from the same animal with 1.9% engraftment in bone marrow. Consistent results were obtained for another 1.9%-engraftment animal. The mineralization was evaluated from the intensity ratio of mineral phosphate ($\nu_1PO_4^{3-}$) to organic CH Raman peaks, mean (± standard error [SE]). The mineralization heterogeneity was defined as the coefficient of variation of the ratio, COV = 100% SD/mean; the mean square errors of COV (mse) were calculated from the mean square error for the unbiased variance estimator.[51]

Perspectives and challenges

The encouraging results obtained in this and previous transplantation studies[10-17] offer hope for an effective cell therapy of patients with OI and other skeletal dysplasias. Still, many questions remain to be answered before such a treatment becomes a reality. Consistent with earlier reports,[15,50] we observed large variations in the engraftment of transplanted cells from animal to animal. Although this could be caused by technical errors due to the small size of mouse embryos, we still do not know which, if any, factors could contribute to determining the level of engraftment and how we may improve it. The engrafted cells were viable at least through the most critical prepubertal development of the animals. A careful study of longer lasting treatment benefits in older mice is substantially more challenging because of several confounding factors (eg, smaller phenotypic difference between untreated BrtlIV and WT animals and effects of improved prepubertal gait and bone mechanics on postpubertal bone development[42]). Initial preliminary observations suggest that there is no statistically significant decrease in the bone marrow engraftment in 4-month-old animals, but much more work remains to be done. To our knowledge, this is the first simultaneous evaluation of the engraftment in mutant OI mice and their WT littermates. Because of the high levels of variability, we did not find a statistically significant difference between BrtlIV and WT littermates, but a trend toward a lower engraftment in mutants suggested that further studies on the effects of endogenous environment on donor cells may help to solve the problem of low and inconsistent engraftment. Similar changes in bone geometry after IUT in BrtlIV and WT littermates raise the possibility of systematic investigation of the potential role of donor humoral factors. In this respect, it may be interesting to compare the cell function and matrix created by BrtlIV and WT cells in all possible combinations of transplanted cells and host animals. These are just few examples of questions to be addressed by future transplantation studies, some of which are currently being conducted by our team.

Acknowledgments

We thank Dr Patrizia Vaghi (Centro Grandi Strumenti, University of Pavia, Italy) for technical assistance and Dr Rosti Vittorio, Department of Molecular and Cell Biology, S. Matteo Hospital, Pavia, Italy for careful reading of the manuscript and suggestions on analysis of hematopoietic cell lineages. C.P. is a PhD student attending the PhD Program in "Biomolecular Sciences and Biotechnologies" of the University of Pavia, Italy.

This work was supported by MIUR 2006 (2006050235), Consorzio Interuniversitario Biotecnologie (C.I.B.), Progetto Regione Lombardia-Università "Dalla Scienza dei Materiali alla Biomedicina Molecolare," Fondazione Cariplo grant to A. Forlino, Fondazione Cariplo N.O.B.E.L. Project to P.V., European Community (FP6, LSHM-CT-2007-037471), Intramural Research Program of the NIH, NICHD and NIH Director's Challenge Fund.

Authorship

Contribution: A. Forlino, A. Frattini, and P.V. designed the study; C.P., R.G, A.L., R.B., J.K., J.C.V., E.L.M., E.P., F.B., I.V., A. Farina, M.C., and A. Forlino performed the experiments; C.P., S.A.G., E.L.M., S.L., G.C., A.R., P.V., and A. Forlino analyzed the data; and S.A.G., S.L., J.C.M., and A. Forlino wrote the paper.

Conflict-of-interest disclosure: The authors declare no competing financial interests.

Correspondence: Antonella Forlino, Department of Biochemistry "A. Castellani," Section of Medicine and Pharmacy, University of Pavia, Via Taramelli 3/B, 27100 Pavia, Italy; e-mail: aforlino@unipv.it.

References

1. Prockop DJ. Marrow stromal cells as stem cells for nonhematopoietic tissues. *Science.* 1997;276:71-74.
2. Byers PH, Cole GC. Osteogenesis imperfecta. In: Royce PM, Steinmann B, eds. Connective Tissue and its Heritable Disorders. 2nd Ed. New York, NY: Wiley-Liss; 2002:385-430.
3. Kuivaniemi H, Tromp G, Prockop DJ. Mutations in collagen genes: causes of rare and some common diseases in humans. *FASEB J.* 1991;5: 2052-2060.
4. Antoniazzi F, Mottes M, Fraschini P, Brunelli PC, Tato L. Osteogenesis imperfecta: practical treatment guidelines. *Paediatr Drugs.* 2000;2:465-488.
5. Fleisch H. Bisphosphonates: mechanisms of action. *Endocr Rev.* 1998;19:80-100.
6. Rauch F, Glorieux FH. Treatment of children with osteogenesis imperfecta. *Curr Osteoporos Rep.* 2006;4:159-164.
7. Millington-Ward S, McMahon HP, Farrar GJ. Emerging therapeutic approaches for osteogenesis imperfecta. *Trends Mol Med.* 2005;11: 299-305.
8. Chamberlain JR, Deyle DR, Schwarze U, et al. Gene targeting of mutant COL1A2 alleles in mesenchymal stem cells from individuals with osteogenesis imperfecta. *Mol Ther.* 2008;16:187-193.
9. Cabral WA, Marini JC. High proportion of mutant osteoblasts is compatible with normal skeletal function in mosaic carriers of osteogenesis imperfecta. *Am J Hum Genet.* 2004;74:752-760.
10. Horwitz EM, Prockop DJ, Gordon PL, et al. Clinical responses to bone marrow transplantation in children with severe osteogenesis imperfecta. *Blood.* 2001;97:1227-1231.
11. Horwitz EM, Prockop DJ, Fitzpatrick LA, et al. Transplantability and therapeutic effects of bone marrow-derived mesenchymal cells in children with osteogenesis imperfecta. *Nat Med.* 1999;5: 309-313.
12. Horwitz EM, Gordon PL, Koo WK, et al. Isolated allogeneic bone marrow-derived mesenchymal cells engraft and stimulate growth in children with osteogenesis imperfecta: implications for cell therapy of bone. *Proc Natl Acad Sci U S A.* 2002; 99:8932-8937.
13. Le Blanc K, Gotherstrom C, Ringden O, et al. Fetal mesenchymal stem-cell engraftment in bone

after in utero transplantation in a patient with severe osteogenesis imperfecta. *Transplantation.* 2005;79:1607-1614.

14. Pereira RF, O'Hara MD, Laptev AV, et al. Marrow stromal cells as a source of progenitor cells for nonhematopoietic tissues in transgenic mice with a phenotype of osteogenesis imperfecta. *Proc Natl Acad Sci U S A.* 1998;95:1142-1147.
15. Li F, Wang X, Niyibizi C. Distribution of single-cell expanded marrow derived progenitors in a developing mouse model of osteogenesis imperfecta following systemic transplantation. *Stem Cells.* 2007;25:3183-3193.
16. Guillot PV, Abass O, Bassett JH, et al. Intrauterine transplantation of human fetal mesenchymal stem cells from first-trimester blood repairs bone and reduces fractures in osteogenesis imperfecta mice. *Blood.* 2008;111:1717-1725.
17. Wang X, Li F, Niyibizi C. Progenitors systemically transplanted into neonatal mice localize to areas of active bone formation in vivo: implications of cell therapy for skeletal diseases. *Stem Cells.* 2006;24:1869-1878.
18. Phinney DG, Prockop DJ. Concise review: mesenchymal stem/multipotent stromal cells: the state of transdifferentiation and modes of tissue repair—current views. *Stem Cells.* 2007;25:2896-2902.
19. Pihlajaniemi T, Dickson LA, Pope FM, et al. Osteogenesis imperfecta: cloning of a pro-alpha 2(I) collagen gene with a frameshift mutation. *J Biol Chem.* 1984;259:12941-12944.
20. Forlino A, Porter FD, Lee EJ, Westphal H, Marini JC. Use of the Cre/lox recombination system to develop a nonlethal knock-in murine model for osteogenesis imperfecta with an α1(I) G349C substitution. Variability in phenotype in BrtlIV mice. *J Biol Chem.* 1999;274:37923-37931.
21. Engel J, Prockop DJ. The zipper-like folding of collagen triple helices and the effects of mutations that disrupt the zipper. *Annu Rev Biophys Biophys Chem.* 1991;20:137-152.
22. Ying QL, Wray J, Nichols J, et al. The ground state of embryonic stem cell self-renewal. *Nature.* 2008;453:519-523.
23. Chambers I, Smith A. Self-renewal of teratocarcinoma and embryonic stem cells. *Oncogene.* 2004;23:7150-7160.
24. Burdon T, Smith A, Savatier P. Signalling, cell cycle and pluripotency in embryonic stem cells. *Trends Cell Biol.* 2002;12:432-438.
25. Choumerianou DM, Dimitriou H, Kalmanti M. Stem cells: promises versus limitations. *Tissue Eng Part B Rev.* 2008;14:53-60.
26. Pittenger MF, Mackay AM, Beck SC, et al. Multilineage potential of adult human mesenchymal stem cells. *Science.* 1999;284:143-147.
27. Ferrari G, Cusella-De Angelis G, Coletta M, et al. Muscle regeneration by bone marrow-derived myogenic progenitors. *Science.* 1998;279:1528-1530.
28. Bianco P, Robey PG, Simmons PJ. Mesenchymal stem cells: revisiting history, concepts, and assays. *Cell Stem Cell.* 2008;2:313-319.
29. Flake AW, Zanjani ED. In utero hematopoietic stem cell transplantation: ontogenic opportunities and biologic barriers. *Blood.* 1999;94:2179-2191.
30. Peranteau WH, Hayashi S, Kim HB, Shaaban AF, Flake AW. In utero hematopoietic cell transplantation: what are the important questions? *Fetal Diagn Ther.* 2004;19:9-12.
31. Hayashi S, Peranteau WH, Shaaban AF, Flake AW. Complete allogeneic hematopoietic chimerism achieved by a combined strategy of in utero hematopoietic stem cell transplantation and postnatal donor lymphocyte infusion. *Blood.* 2002; 100:804-812.
32. Okabe M, Ikawa M, Kominami K, Nakanishi T, Nishimune Y. 'Green mice' as a source of ubiquitous green cells. *FEBS Lett.* 1997;407:313-319.
33. Dobson KR, Reading L, Haberey M, Marine X, Scutt A. Centrifugal isolation of bone marrow from bone: an improved method for the recovery and quantitation of bone marrow osteoprogenitor cells from rat tibiae and femurae. *Calcif Tissue Int.* 1999;65:411-413.
34. Peister A, Mellad JA, Larson BL, Hall BM, Gibson LF, Prockop DJ. Adult stem cells from bone marrow (MSCs) isolated from different strains of inbred mice vary in surface epitopes, rates of proliferation, and differentiation potential. *Blood.* 2004; 103:1662-1668.
35. Frattini A, Blair HC, Sacco MG, et al. Rescue of ATPa3-deficient murine malignant osteopetrosis by hematopoietic stem cell transplantation in utero. *Proc Natl Acad Sci U S A.* 2005;102: 14629-14634.
36. Uveges TE, Collin-Osdoby P, Cabral WA, et al. Cellular mechanism of DECREASED Bone in Brtl mouse model of OI: imbalance of decreased osteoblast function and increased osteoclasts and their precursors. *J Bone Miner Res.* 2008;6:6.
37. Bilic-Curcic I, Kronenberg M, Jiang X, et al. Visualizing levels of osteoblast differentiation by a two-color promoter-GFP strategy: type I collagen-GFPcyan and osteocalcin-GFPtpz. *Genesis.* 2005;43:87-98.
38. Kucia M, Reca R, Jala VR, Dawn B, Ratajczak J, Ratajczak MZ. Bone marrow as a home of heterogenous populations of nonhematopoietic stem cells. *Leukemia.* 2005;19:1118-1127.
39. Laird PW, Zijderveld A, Linders K, Rudnicki MA, Jaenisch R, Berns A. Simplified mammalian DNA isolation procedure. *Nucleic Acids Res.* 1991;19: 4293.
40. Robey PG, Termine JD. Human bone cells in vitro. *Calcif Tissue Int.* 1985;37:453-460.
41. Forlino A, Tani C, Rossi A, et al. Differential expression of both extracellular and intracellular proteins is involved in the lethal or nonlethal phenotypic variation of BrtlIV, a murine model for osteogenesis imperfecta. *Proteomics.* 2007;7:1877-1891.
42. Kozloff KM, Carden A, Bergwitz C, et al. Brittle IV mouse model for osteogenesis imperfecta IV demonstrates postpubertal adaptations to improve whole bone strength. *J Bone Miner Res.* 2004;19:614-622.
43. Dominici M, Marino R, Rasini V, et al. Donor cell-derived osteopoiesis originates from a self-renewing stem cell with a limited regenerative contribution after transplantation. *Blood.* 2008; 111:4386-4391.
44. Baena E, Ortiz M, Martinez AC, de Alboran IM. c-Myc is essential for hematopoietic stem cell differentiation and regulates Lin(-)Sca-1(+)c-Kit(-) cell generation through p21. *Exp Hematol.* 2007; 35:1333-1343.
45. Uveges TE, Bergwitz C, Kozloff KM, et al. Homozygosity for a dominant negative type I collagen mutation attenuates the type IV OI phenotype of the heterozygous Brtl mouse: insight into desease mechanism. *Bone.* 2005;36:S128-S129.
46. Kuznetsova NV, Forlino A, Cabral WA, Marini JC, Leikin S. Structure, stability and interactions of type I collagen with GLY349-CYS substitution in α1(I) chain in a murine osteogenesis imperfecta model. *Matrix Biol.* 2004;23:101-112.
47. Martin RB, Burr BB, Sharkey NA. *Skeletal Tissue Mechanics.* New York, NY: Springer; 1998.
48. Forlino A, Kuznetsova NV, Marini JC, Leikin S. Selective retention and degradation of molecules with a single mutant α1(I) chain in the Brtl IV mouse model of OI. *Matrix Biol.* 2007;26:604-614.
49. Prockop DJ. "Stemness" does not explain the repair of many tissues by mesenchymal stem/multipotent stromal cells (MSCs). *Clin Pharmacol Ther.* 2007;82:241-243.
50. Guillot PV, Gotherstrom C, Chan J, Kurata H, Fisk NM. Human first-trimester fetal MSC express pluripotency markers and grow faster and have longer telomeres than adult MSC. *Stem Cells.* 2007;25:646-654.
51. Mood A, Graybill F, Boes D. *Introduction to the Theory of Statistics.* 3rd ed. New York, NY: McGraw-Hill; 1974.